Available online at www.sciencedirect.com

ScienceDirect

journal homepage: www.elsevier.com/locate/he

Options for net zero emissions hydrogen from Victorian lignite. Part 2: Ammonia production

M.A. Kibria [a], D.E. McManus [b,**], S. Bhattacharya [a,*]

[a] Monash University, Department of Chemical and Biological Engineering, PO Box 36, Clayton Victoria 3800, Australia

[b] Australian Carbon Innovation, Building 4W-127 Federation University Gippsland, Churchill, Victoria 3842, Australia

HIGHLIGHTS

- A detailed model for net-zero emissions ammonia from Victorian lignite proposed.
- Gasification of lignite, production of ammonia and electricity, with CCS included.
- Power consumption for liquefaction of 32.4 t h^{-1} hydrogen or conversion to ammonia surprisingly similar.
- Production of ammonia from Victorian lignite with net-zero emissions is feasible.
- Direct comparison with resource requirements for the production of green ammonia.

GRAPHICAL ABSTRACT

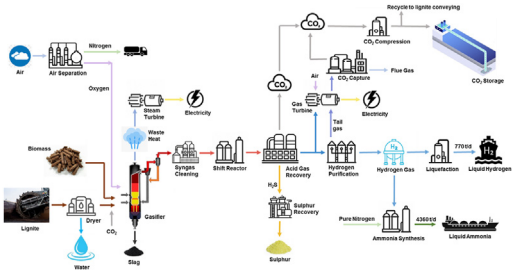

ARTICLE INFO

Article history:
Received 22 January 2023
Received in revised form
6 May 2023
Accepted 9 June 2023
Available online 26 June 2023

Keywords:
Ammonia
Lignite
Gasification
Carbon capture

ABSTRACT

This the second of a two-part study investigating the feasibility of producing export quantities (770 t/d) of blue hydrogen meeting international emissions standards, by gasification of Victorian lignite plus carbon capture and storage (CCS). Part 1 focussed on the resources, energy requirements, and greenhouse gas emissions associated with the production of gaseous and liquefied hydrogen, while Part 2 focusses on the production of ammonia as an alternative hydrogen carrier for export.

In this study, an Aspen Plus simulation of a conventional 1500 t d^{-1} iron-based catalyst Haber-Bosch ammonia synthesis process is developed and incorporated into the earlier lignite-to-hydrogen process model. Development of the simulation involves (i) estimation of the instantaneous rate kinetics, (ii) calibration against test data for a reactor of known dimensions, (iii) scaling up the bed dimensions to achieve a target production capacity, (iv) selecting an appropriate feed gas composition to optimise performance, (v) adjusting purge

* Corresponding author.
** Corresponding author.
E-mail addresses: dmcmanus@acinnovation.com.au (D.E. McManus), sankar.bhattacharya@monash.edu (S. Bhattacharya).

https://doi.org/10.1016/j.ijhydene.2023.06.098

Renewable energy
Greenhouse gas intensity

gas flowrates to achieve stable operation, and (v) incorporation into the previous lignite-to-hydrogen simulation.

This study finds that 178.2 t h^{-1} liquid ammonia and all electricity required to support the process can be produced from 1050 t h^{-1} Victorian lignite. Surprisingly, the simulation results show that the electrical power requirement for ammonia synthesis (176.4 MW) is essentially the same as that needed for liquefaction of an equivalent output of hydrogen (175.5 MW). On this basis both options are equally attractive, although ammonia synthesis is at a higher level of technological maturity than large-scale hydrogen liquefaction.

This is the first study to quantify the greenhouse gas emissions intensity of ammonia production from lignite, accounting for the full production chain from lignite mining to CO_2 sequestration. It is found that ammonia can be produced from Victorian lignite with very low CO_2 emission intensity (0.49 $kg_{CO2\text{-}e}$ kg_{NH3}^{-1}) equivalent to that of next-generation natural gas reforming with CCS processes. If required, the emission intensity can be reduced to 0.05$kg_{CO2\text{-}e}$ kg_{NH3}^{-1} with a post-combustion CO_2 capture system, and then made carbon neutral by co-gasification with $\leq$1.4% biomass.

For comparison, this study also examines the implications of producing the same quantity of green ammonia using renewable energy alone. It is estimated that production of 178.2 t h^{-1} green ammonia would require 1946 MW renewable energy and associated transmission infrastructure. In Victoria, this could be supplied by a wind farm with a 5.4 GW rated capacity, occupying an area of over 72,000 ha. This is highly unlikely to be a viable option.

This analysis indicates that clean hydrogen in the form of ammonia, produced in Victoria by lignite gasification with CCS, can be consistent with global emissions reductions targets over the next few decades. The unique combination of low-cost lignite and high-quality CO_2 storage geology means that Victoria is well placed to become a significant exporter of low-emissions ammonia to the world market. Further research is recommended on recovery of energy from the low grade waste heat streams and opportunities for additional electricity generation using the organic Rankine cycle.

Nomenclature

Acronyms

ASU	Air Separation Unit
CCS	Carbon Capture and Storage
EOR	Enhanced Oil Recovery
HESC	Hydrogen Energy Supply Chain
LHV	Lower Heating Value
PEM	Proton Exchange Membrane
PSA	Pressure Swing Adsorption
RO	Reverse Osmosis
SEC	Specific Energy Consumption
SEI	Specific Emissions Intensity
SMR	Steam Methane Reforming

Chemicals

CH_4	Methane
CO_2	Carbon dioxide
CO_2-e	Carbon dioxide equivalent
DEPG	Dimethylether polyethylene glycol
H_2	Hydrogen
H_2S	Hydrogen sulphide
MDEA	Methyldiethanolamine
MCH	Methylcyclohexane
N_2	Nitrogen
NH_3	Ammonia
Selexol™	A proprietary blend of DEPG licensed by Honeywell UOP, and the process for its use
UAN	Urea-ammonium nitrate

Introduction

Hydrogen is anticipated to become a major source of clean energy as the world transitions toward a low-emissions economy. As a chemical carrier of energy, hydrogen can play a crucial bridging role in linking sources of clean energy with remote energy users, particularly in the transportation, industrial, heating and power sectors. Hydrogen produced using renewable energy or fossil fuels with carbon capture and storage (CCS) is environmentally benign and can be utilised via direct combustion, co-combustion and fuel cells [1].

The main challenge for hydrogen as a tradeable energy commodity is its low energy density. Hydrogen is a gas at atmospheric temperature and must be converted to liquid form

for bulk transport. Unlike natural gas, which can be transported as a liquid at −169 °C [2], hydrogen must be cooled to −253 °C which is very energy intensive [3]. Nevertheless, bulk transport of liquid hydrogen is being promoted by the Japanese company Kawasaki Heavy Industries and its collaborators in the Hydrogen Energy Supply Chain (HESC) Project, which envisages a "CO_2 free hydrogen chain" in which low cost blue hydrogen is produced in Australia by gasification of Victorian lignite with CCS, then liquefied and transported to Japan by ship [4,5]. During 2020–2021, the HESC Pilot Project produced hydrogen at 99.999% purity by gasification of lignite and lignite-biomass blends, which was liquefied and successfully transported to Japan on the *Suiso Frontier*, the world's first ocean-going liquid hydrogen carrier ship [6].

Another Japanese company, Chiyoda, has developed an alternative hydrogen supply chain concept based on methylcyclohexane (MCH) as a hydrogen carrier, which is a stable liquid at ambient temperature and pressure. In Chiyoda's SPERA Hydrogen™ process, hydrogen is reacted with toluene to produce MCH which, after transport, is dehydrogenated back to toluene and hydrogen using a proprietary catalyst. The SPERA Hydrogen™ technology has been successfully demonstrated by transporting MCH by sea between a hydrogenation plant in Brunei Darussalam and a dehydrogenation plant in the Kawasaki Coastal Area in Japan [7]. A disadvantage of this approach is that the hydrogenation reaction is highly exothermic, but there is limited scope to make use of the excess energy at the hydrogenation plant. On the other hand, the dehydrogenation reaction is endothermic, requiring a suitable source of renewable energy at the destination site. Also, the recovered toluene must be recycled by sea transport back to the hydrogenation plant, representing an additional energy penalty and source of greenhouse gas emissions [8].

Ammonia is rapidly emerging is a more advantageous hydrogen carrier than either liquefied hydrogen or MCH. Ammonia can be liquefied at 25 °C when pressurized to 1.0 MPa, or at −33.4 °C at atmospheric pressure, and has an energy density approximately double that of liquid hydrogen [9]. Ammonia can be directly used as fuel without CO_2 emissions, and NO_X emissions in ammonia combustion can be controlled. While ammonia has acute toxicity (but no chronic toxicity) with strong smell, it is easy to detect and safety measures are common practice [10]. In Japan, leading power companies, manufacturers and research institutes are collaborating toward commercialization of a CO_2-free ammonia value chain, with significant achievements in development of ammonia-fuelled gas turbine power plant, a direct ammonia-fuelled solid oxide fuel cell, and co-firing of ammonia at a commercial coal power plant [10].

Ammonia is already one of the most important industrial chemicals in the world, with the lives of around half of humanity being dependent on ammonia-based fertilisers. In 2020, 185 million tonnes of ammonia was produced and around 20 million tonnes was traded globally, so the infrastructure to support safe and reliable storage, distribution and export of ammonia is already highly developed. Around 70% of ammonia is used to make fertilisers, with the remainder used for a wide range of industrial applications, such as plastics, explosives and synthetic fibres [11].

Ammonia is produced commercially using the Haber-Bosch process, in which hydrogen is catalytically reacted with nitrogen at high temperatures (typically 400–450 °C) and high pressures (typically 15–25 MPa). The majority (72%) of modern ammonia plants are based on steam methane reforming (SMR) of natural gas, 26% on coal gasification, about 1% on oil products, and a fraction of a percentage point on electrolysis. There are currently around 550 ammonia plants operating globally, ranging in capacity from around 200 kt y^{-1} to 1,200 kt y^{-1}, generating cumulative CO_2 emissions of around 450 Mt y^{-1} [12]. Zhang et al. [13] reported the specific emissions intensity (SEI) of the large ammonia plants in China as 9.0 $kg_{CO2\text{-}e}$ kg_{NH3}^{-1} for coal and 3.0 $kg_{CO2\text{-}e}$ kg_{NH3}^{-1} for SMR. However, Stocks et al. [14] estimated that the total emissions intensity of SMR (including fugitive emissions) could be reduced to 0.44–0.54 $kg_{CO2\text{-}e}$ kg_{NH3}^{-1} by employing CCS with 90% CO_2 capture.

In Part 1 of this study, we developed an Aspen Plus simulation model for production of blue hydrogen by gasification of Victorian lignite plus CCS [15]. The individual unit operations were validated against published industrial data to ensure that the simulation was as realistic as possible. It was shown that 770 t d^{-1} liquefied hydrogen and all required electricity could be co-produced with a specific emissions intensity of 2.73 $kg_{CO2\text{-}e}$ kg_{H2}^{-1}, including upstream fugitive methane emissions. This conforms to the current EU Taxonomy limit of 3.0 $kg_{CO2\text{-}e}$ kg_{H2}^{-1} for 'sustainable' hydrogen. It was also shown that the SEI can be reduced to 0.3 $kg_{CO2\text{-}e}$ kg_{H2}^{-1} by addition of a post-combustion CO_2 capture unit, and to net-zero or net-negative by co-gasification with biomass. The concept of producing blue hydrogen by gasification of Victorian lignite plus CCS is thus consistent with policy settings of 'net zero by 2050'.

In Part 2, we extend this analysis to investigate the relative merits of converting the same quantity of gaseous hydrogen to ammonia rather than liquefied hydrogen. In principle, if less energy is required to convert the hydrogen to ammonia than for liquefaction, the CO_2 emissions and cost would both be reduced. To conduct this study on a like-for-like basis, the simulated ammonia synthesis process must be based on industrially-validated design data, as in the previous study. This is challenging, however, because publication of commercially-sensitive ammonia plant design and performance data is typically restricted. As such, there is very little relevant data available in the public domain.

The key to ammonia reactor design is the catalyst reaction kinetics. The conventional Haber-Bosch process uses iron-based catalysts, which are equilibrium-limited with typically 20–30% conversion efficiency per pass, requiring large reactor volumes to achieve good economics. Alternative catalysts have been developed for operation under milder conditions, e.g., ICI's cobalt-modified magnetite catalyst and Kellog's ruthenium catalyst, but they do not significantly improve the process economics [16].

Some conceptual studies of potential low-emissions ammonia production schemes make the simplifying assumption that equilibrium is achieved within the synthesis reactor, e.g., Refs. [17–21]. In reality, however, ammonia synthesis is equilibrium-limited, so this approach overestimates the reaction temperatures and underestimates the

energy requirement. A rate-based modelling approach is needed to more accurately simulate the performance of a commercial process.

The most widely used rate expression used to characterise performance of iron-based catalysts is the modified Temkin equation, which is a correlation based on laboratory rate data for the widely-used Haldor Topsøe KM1 catalyst. This equation has been successfully used in one-dimensional analytical models [23–25] to simulate the performance of industrial Haber-Bosch ammonia synthesis reactors. Araújo and Skogestad [26] developed an Aspen Plus model using modified Temkin reaction kinetics to develop a control strategy for an industrial ammonia plant in Germany. While the model was based on industrial data, no design details of the plant were published. Yoshida et al. [27] used Aspen Plus simulation to compare the economies of scale for ammonia production using either iron- or ruthenium-based catalysts. Based on laboratory rate kinetics, it was found that iron-based catalysts offer lowest production costs at scales of more than 100 t d^{-1}, while ruthenium-based catalysts are more economical at smaller scales. Rossetti et al. [28] developed an Aspen Plus simulation for a process to produce hydrogen from waste biomass and conversion to liquid ammonia, using a combination of both iron-based and ruthenium-based catalysts. In this case, the rate equations were validated against micro-pilot plant data. El-Gharbawy et al. [29] used the modified Temkin equation in an Aspen HYSYS simulation of a commercial ammonia plant in Egypt. Industrial plant test data was used to validate a novel correlation for the equilibrium constant. This is the only known report where industrial ammonia plant design details, plant test data and vendor simulation data have all been published.

While most ammonia is produced from natural gas using SMR, about one quarter is produced by gasification of coal. In 1980, Haldor Topsøe announced development of a coal-to-ammonia process based on a Texaco slurry-feed gasifier. In this process, shift conversion was done in two stages, using a sulphur-tolerant shift catalyst. Hydrogen sulphide and carbon dioxide were then removed in an acid gas removal unit, and remaining carbon oxides were removed by methanation before ammonia synthesis in an iron-based catalytic reactor [30]. In 1984, the Japanese company Ube Corporation commissioned a 1000 t d^{-1} coal-to-ammonia plant based on this process, which is still operational today [31]. The biomass-to-ammonia simulation developed by Rossetti et al. [28] is also based on the same process concept. Stork et al. [32] examined the economic feasibility of co-producing ammonia and electricity from coal was assessed. However, no simulation modelling of this process was published.

In 2011, the U.S. National Energy Technology Laboratory published a feasibility study on a coal-to-hydrogen process incorporating CO_2 capture [33]. The process included oxygen-blown slurry-feed gasification, sour water-gas shift reaction, two-stage Selexol™ acid gas removal and hydrogen purification using pressure swing adsorption (PSA). An Aspen Plus model was developed to assist in sizing the equipment for cost estimation, but no details were published. This process was the basis for Part 1 of our study, where we developed a detailed Aspen Plus simulation for production of 32.4 t h^{-1} low emissions hydrogen from Victorian lignite [15].

The main objective of Part 2 of this study is to extend our model to include the Haber-Bosch process to convert the produced hydrogen to ammonia, and to compare the resource requirements and CO_2 emissions intensity of export-scale production of either liquefied hydrogen or ammonia from Victorian lignite with CCS. To accomplish this, an Aspen Plus process model for ammonia synthesis is developed, using the published design and test data for a commercial Egyptian ammonia plant [29]. The developed model, scaled for processing 32.4 t h^{-1} hydrogen, is then incorporated into our earlier lignite-to-hydrogen simulation model, allowing estimation of the overall resource requirements and CO_2 emissions intensity of lignite-to-ammonia production.

Model development, calibration and scaleup

Overview of Aspen Plus simulation concept

The lignite-to-hydrogen simulation previously developed [15] comprises lignite mining, lignite drying and milling, air separation unit (ASU), dry-feed entrained flow gasification, gas cooling and cleaning, sour water-gas shift reaction, acid gas removal, pressure swing adsorption (PSA) for hydrogen purification, elemental sulphur recovery, CO_2 compression for transport and injection, steam and gas turbines to generate all process power, plus an optional post-combustion CO_2 capture step. In the present study, the simulation model is extended to include Haber-Bosch ammonia synthesis.

The high-level Aspen Plus flowsheet for the entire lignite-to-ammonia process is depicted in Fig. 1. It can be seen that the AMMONIA Hierarchy block is integrated with the lignite-to-hydrogen process through two input streams and two output streams. The input streams are hydrogen from the PSA and nitrogen from the ASU. The output streams are liquid ammonia and a relatively small purge gas stream that is sent for combustion in the gas turbine block, to extract energy and prevent atmospheric release of waste gases.

The Aspen Plus flowsheet of the AMMONIA Hierarchy block (Fig. 2) comprises three main sections: the compression system, the synthesis reactor, and the cooling unit. The feed streams into the AMMONIA Hierarchy block are ultrapure gaseous hydrogen and nitrogen. Hydrogen at 99.999% purity is produced in the PSA unit 15 °C, 2.75 MPa, at the rate of 32.4 t h^{-1}. Nitrogen at >99.9% purity is extracted from the top of the high pressure column of the ASU at −177 °C, 0.58 MPa [34,35]. To handle the feed of 32.4 t h^{-1} hydrogen, the ammonia synthesis system is conceived as three separate systems operating in parallel. Each individual system has an ammonia production capacity of around 1500 t d^{-1}, which is typical for large commercial ammonia facilities [16]. A single such unit is represented in Fig. 2, with splitters, duplicators and mixers replicating the other two units in parallel. To initialise the simulation, it is necessary for there to be a low but non-zero feed of NH_3 into the system to prevent the reaction rate equation (Eq. (2), Section 2.2 below) going to infinity.

The core of the AMMONIA Hierarchy block is the ammonia synthesis reactor, representing the conventional Haber-Bosch process with Haldor Topsøe iron-based KM1 catalyst. The exothermic reaction is conducted at 400–500 °C temperature

and 17.1 MPa pressure. Each synthesis reactor comprises three catalyst beds with two intercooling stages, which is the most efficient design in terms of ammonia production, energy savings, capital, and maintenance cost [16]. In Aspen Plus, the catalyst beds are represented by RPlug adiabatic plug flow reactors. Within each RPlug block, the instantaneous reaction rate is calculated as a function of position, temperature, and pressure. The procedure for calculating the instantaneous reaction rate, gas composition and temperature is described in Section 2.2. The simulation is calibrated against industrial plant data to account for diffusion limitations and catalyst ageing (described in Section 2.3) and the catalyst bed dimensions are scaled up to a capacity of 1500 t d^{-1} (Section 2.4). The ammonia synthesis reaction is inhibited by the high temperatures involved, so unreacted gases are recycled in a loop to boost the conversion efficiency.

In the Egyptian industrial plant, temperature control of the catalyst beds is achieved using two interbed heat exchangers, which preheat incoming feed gas against the hot gas exiting beds 1 and 2, plus controlled injection of feed gas directly into the reactor as quench streams [29]. This arrangement allows the temperature profile within the reactor to be maintained without any external heating or cooling load. To simplify calculations in the Aspen Plus model, the temperature profile is adjusted using two inter-bed heat exchangers, with dummy heat loads that do not connect with the rest of the plant.

Reaction gas exits the synthesis reactor at 452 °C and must be chilled to condense and separate the ammonia product. There is limited information in the literature on the conditions used industrially to condense ammonia. Araújo and Skogestad [26] describe an industrial plant where ammonia is condensed at 40.5 °C and 19.6 MPa, but this pressure is higher than that used in the present model. Zhang et al. [36] provide details of a state-of-the-art Chinese methane-to-ammonia plant in which ammonia condensation is accomplished through two flash cooling steps. The first stage operates at −5 °C and 16 MPa, and the second operates at −3 °C and 2.5 MPa, producing liquid NH_3 product at 99.8 mol% purity. The same approach is adopted in the present model. Operation of FLASH1 at 16 MPa is readily synchronised with the reactor pressure, while operation of FLASH2 at 2.5 MPa is convenient for transportation purposes.

The cooling unit also includes five heat exchangers which reduce the temperature of the gas stream prior to ammonia separation. WC1 uses water to raise steam and cool the gas from 452 °C to 232 °C. Air cooler AIR cools the gas to 150 °C, then WC2 uses water to cool the gas to 20 °C. In ASU1, a portion of nitrogen from the ASU at −177 °C cools the gas to −5 °C before FLASH1. In ASU2, a second portion of nitrogen cools the gas to −3 °C before FLASH2. After passing through ASU1 and ASU2 the nitrogen is at 15 °C, ready for compression in COMP1. A total of 123 MW of cooling energy is required, with 52 MW_{th} extracted in WC1 and 17 MW_{th} extracted in ASU1 and ASU2.

To prevent accumulation of the impurities in the H_2 and N_2 feed streams under continuous recycle, it is necessary to purge a portion of the recycle stream. Due to the high purity of the reactant gases, a purge of around 1% of the recycle gas suffices. This is extracted from the vapour phase from FLASH1 at splitter SPL3. The vapour phase outlet from FLASH2, which is predominantly nitrogen, is also sent to the gas turbine.

In the compression system, COMP1 boosts the pressure of the H_2 and N_2 feed streams to the reaction pressure of 17.1 MPa. COMP2 is used to boost the recycle gas stream back up to reaction pressure. COMP3 is a small compressor used to match the pressure of the purge gas from FLASH2 (2.5 MPa) with that of FLASH1 (16 MPa), before they are combined and sent to the gas turbine for combustion. At the gas turbine, the gas stream is preheated and expanded to synchronize with the turbine operating conditions. Further details of the elements within the AMMONIA Hierarchy block are presented in Table 1, and a description of each of the numbered streams is provided in Table 2.

Quantifying the energy intensity of ammonia synthesis requires a realistic model of a typical industrial-scale synthesis plant, validated by test data. The following sections describe the process followed used to develop a representative model based on published data, involving (i) estimation of the instantaneous rate kinetics, (ii) calibration against test data

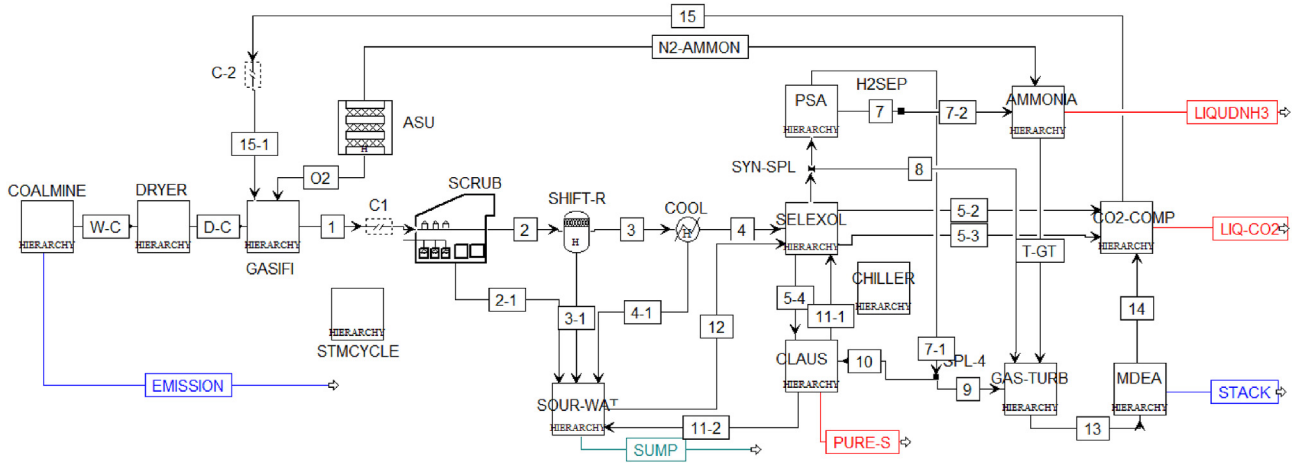

Fig. 1 – High level Aspen Plus process flowsheet for ammonia production from lignite.

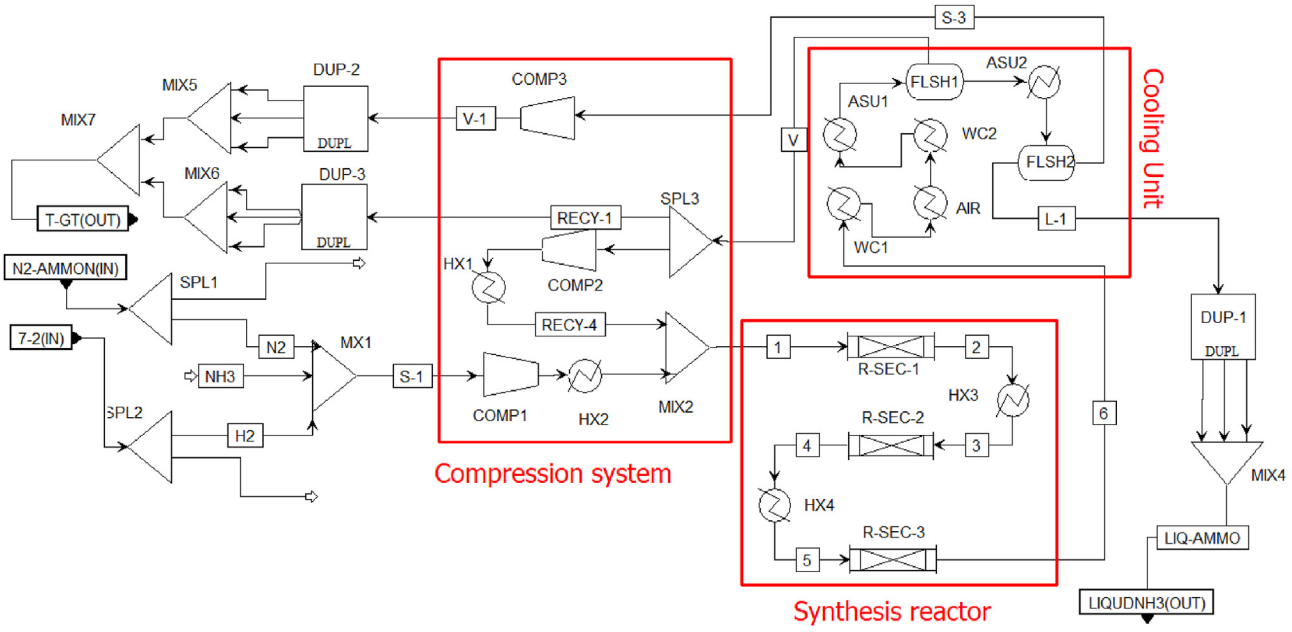

Fig. 2 – Aspen Plus model of the AMMONIA Hierarchy block.

for a reactor of known dimensions, (iii) scaling up the bed dimensions to achieve a target production capacity, (iv) selecting an appropriate feed gas composition to optimise performance, (v) adjusting purge gas flowrates to achieve stable operation, and (v) incorporation of the developed model into the previous lignite-to-hydrogen Aspen Plus simulation.

Catalyst rate kinetics

The key to ammonia synthesis is the catalyst, which facilitates the reaction of hydrogen with nitrogen to produce ammonia (Eq. (1)).

$$N_2 + 3\,H_2 \leftrightarrow 2\,NH_3 \qquad \Delta H^{o}_{298} = -46\ kJ.mol^{-1}\ NH_3 \tag{1}$$

It is assumed that the catalyst for this reaction is the widely used commercial Haldor Topsøe iron-based KM1 catalyst. The instantaneous reaction rate, r_{NH3}, for ammonia synthesis with this catalyst can be estimated using the modified Temkin expression, following the procedure detailed by Dyson and Simon [22]:

$$r_{NH_3} = k_r \left(K_a^2 a_{N_2} \left[\frac{(a_{H_2})^3}{(a_{NH_3})^2} \right]^{0.5} - \left[\frac{(a_{NH_3})^2}{(a_{H_2})^3} \right]^{0.5} \right) \tag{2}$$

where: r_{NH3} is the instantaneous reaction rate in kmol NH_3.-h^{-1}.m^{-3} of catalyst bed.

k_r is a kinetic constant of the reverse reaction, dimensionless.

K_a is the equilibrium constant of the reaction, dimensionless

a_i ($i = H_2, N_2, NH_3$) is the activity of component i

$$k_r = 1.7698 \times 10^{15} \exp\left(-40765 / R_c T\right) \tag{3}$$

where: R_c is the gas constant, 1.987 cal K^{-1} mol^{-1}

T is temperature, Kelvin

$$log_{10}K_a = -2.691122\ log_{10}T - 5.519265x10^{-5}T + 1.848863x10^{-7}T^2 + 2001.6/T + 2.6899 \tag{4}$$

The activity of each component is given by:

$$a_i = X_i f_i^o \tag{5}$$

where: X_i is the mole fraction of each component.

f_i^o is the pure component fugacity at the temperature and pressure of the system

The fugacity of each pure component is given by:

$$f_i^o = \gamma_i P \tag{6}$$

where: P is the pressure, atm

$$\gamma_{H_2} = \exp\left[e^{\left(-3.8402T^{0.125}+0.541\right)} P - e^{\left(-0.1263T^{0.5}-15.980\right)} P^2 + 300\, e^{\left(-0.011901T-5.941\right)} \left(e^{-P/300} - 1\right) \right] \tag{7}$$

$$\gamma_{N_2} = 0.93931737 + 0.3101804x10^{-3}T + 0.295896x10^{-3}P - 0.2707279x10^{-6}T^2 + 0.4775207x10^{-6}P^2 \tag{8}$$

$$\gamma_{NH_3} = 0.1438996 + 0.2028538x10^{-2}T - 0.4487672x10^{-3}P - 0.1142945x10^{-5}T^2 + 0.2761216x10^{-6}P^2 \tag{9}$$

Using Eqs. (2)–(9), the reaction rate is calculated as a function of position, temperature, and pressure in the catalyst bed. The resulting values represent the instantaneous reaction rate at each point, and have been shown to closely match the performance of powdered Haldor Topsøe KM1 catalyst [16].

In practice, the apparent reaction rate is substantially lower than the instantaneous reaction rate, due to the

Table 1 – AMMONIA Hierarchy block description and operating conditions.

Block ID	Aspen Block	Purpose	Specification
SPL-1,2	Splitter	To split incoming N_2 and H_2	Both 0.333
MIX-1-7	Mixer	To mix incoming stream	Adiabatic
COMP-1,2,3	Compressor	To compress N_2 and H_2 mixture	Discharge pressure 17.1 MPa(a)
HX-1-4	Heater block	To cool material stream	HX-1,2: T-394 °C, P-0 MPa HX-3: T-434 °C, P-0 MPa HX-4: T-413 °C, P-0 MPa
WC1-2 AIR ASU1-2	Heater block	To cool material stream	WC1: T-232 °C, P-0 MPa WC2: T-20 °C, P-0 MPa AIR: T-150 °C, P-0 MPa ASU1: T-(-3 °C), P-0 MPa ASU2: T-(-3 °C), P-0 MPa
R-SEC-1,2,3	RPlug	Kinetic reactor	Adiabatic Pressure drop - Ergun Catalyst: Diameter 2.3 mm, Density 2.3 g/ml
FLSH1-2	Flash	To flash the incoming stream by cooling and reducing pressure	FLSH1: T-(-5 °C), P-16 MPa FLSH2: T-(-3 °C), P-2.5 MPa
DUP-1-3	Duplicator	To duplicate material stream	Each 3

combined effects of diffusional limitations within the catalyst pellets and deactivation of catalyst over time. A pore effectiveness factor, ξ, defined as the ratio of the actual reaction rate to the intrinsic reaction rate, is used as a correction factor for engineering design of ammonia converters [16]. Dyson and Simon [22] derived an expression for ξ from first principles, and then used the results of numerous calculations to develop an empirical expression for ξ in terms of P, T and η, with η defined as the conversion of nitrogen as measured for a reference mixture ($\eta = 0$) containing 3:1H_2/N_2 ratio and 12.7% inert. Elnashaie et al. [37,38] found that the empirical expression provided the best fit to plant data, but it was necessary to further modify the reaction rate by a factor of 0.75 to properly account for deactivation of aged catalyst [37].

In the present case, the concentration of inert gases is very low, so the empirical expression of Dyson and Simon is not applicable. The results of [37] suggest that, provided suitable plant data is available for validation, it is not necessary to calculate ξ and then estimate a second factor to account for catalyst deactivation. Instead, simulation data based on the instantaneous reaction rate, r_{NH3}, can be directly correlated with plant data to estimate an apparent effectiveness factor, β, which includes the effects of both diffusional limitations and catalyst aging. This is the approach adopted in this study, as described below.

Table 2 – Key to AMMONIA Hierarchy block stream numbering.

Stream Number	Description
7-2(IN)	Ultrapure H_2 at 32.4 t h^{-1}
N2-AMMON(IN)	Ultrapure N_2 from the ASU
NH3	Nominal non-zero flow of NH_3 to stop reaction rate going to infinity
S-1	Blended stream of 1/3 x 7-2(IN), 1/3 x N2-AMMON(IN) and NH3
1	Reactant stream entering the first catalyst bed
2	Product stream exiting the first catalyst bed
3	Reactant stream entering the second catalyst bed
4	Product stream exiting the second catalyst bed
5	Reactant stream entering the third catalyst bed
6	Product stream exiting the third catalyst bed
V	Vapour phase exiting the first flash separator
L	Liquid phase exiting the first flash separator
RECY-1	Purge stream from ammonia reactor recycle loop
RECY-4	Recycle loop stream returning to synthesis reactor
S-3	Vapour phase exiting the second flash separator
V-1	Vapour phase purge S-3 after compression from 2.5 MPa to 16 MPa
T-GT(OUT)	Total purge to gas turbine from 3 synthesis reactors
L-1	Liquid phase exiting the second flash separator
LIQUDNH3(OUT)	Total liquid ammonia product from 3 synthesis reactors

Calibration of model using industrial plant data

The instantaneous reaction rate, r_{NH3}, for ammonia synthesis is dependent on the composition of the gas stream and temperature at each point in the catalyst bed (Eqs. (2)–(9)), varying across the bed width. To emulate the performance of an operating industrial plant, the instantaneous reaction rate is modified by an apparent effectiveness factor, β, to match published plant test data. In this case, the industrial data is for a state-of-the-art Uhde ammonia synthesis reactor comprising three catalyst beds with inter-bed cooling. The reactor is a cylindrical vessel, about 20 m high with an internal diameter of 2.8 m, containing three beds of 1.5–3 mm iron-based catalyst. The catalyst beds are of radial-flow configuration, with an external diameter of approximately 2.5 m and bed depth of 0.602 m, 0.694 m and 0.916 m for the 1st, 2nd and 3rd beds, respectively [29]. To simulate radial-flow conditions,

Table 3 – Catalyst bed dimensions and apparent effectiveness factor, β

Reactor Bed	Volume, m^3	Bed Depth, m	Equiv. Diameter, m	Void Fraction	Residence Time, s	β
1	17.46	0.602	6.077	0.241	8.18	0.5
2	13.43	0.694	4.964	0.241	5.28	0.7
3	20.96	0.916	5.398	0.225	8.68	0.7

each bed is modelled as a short, large diameter cylinder, with a cumulative gas path length of 2.21 m through the reactor. The catalyst bed dimensions are shown in Table 3, including estimates of the average bulk gas residence time in each catalyst bed, derived from the single-pass industrial field test results shown in Table 4. The simulation model is calibrated to mimic the plant performance by varying the value of β by trial-and-error to achieve the best match with the experimental data. The estimated values of β for each bed are also included in Table 3.

The best-match temperature estimates at the inlet and outlet of each bed, and the final ammonia concentration, are compared with the trial test results in Table 4. Vendor simulation data for the same test results [29] are compared with the present simulation results in Fig. 3. The close match between the ammonia concentrations and temperature profiles within each bed serves to validate the accuracy of the developed simulation model. It can be seen that, under the operating conditions used, the reactor comes close to achieving equilibrium in all beds. The single-pass conversion of hydrogen to ammonia in this case is 27%, consistent with typical commercial experience [16].

Effect of feed composition on ammonia production

From Eq. (1), reaction stoichiometry suggests that a H_2/N_2 molar ratio of 3:1 would be optimal for NH_3 production. However, Eq. (2) indicates that, for constant temperature and pressure, the rate of NH_3 formation is related to the mole fraction of H_2, N_2 and NH_3 in a complex fashion. The influence of the feed H_2:N_2 molar ratio on the reactor performance was investigated by calculating the gas composition profile as a function of distance across Bed 1, maintaining a constant total molar flowrate (26,409 kmol h^{-1}, as in Table 4) and average operating conditions of 450 °C and 17.1 MPa. The mole fraction of NH_3 in the feed gas is constant at 4.8%. The resulting data on H_2 conversion efficiency and NH_3 production as a function of inlet H_2:N_2 ratio is presented in Fig. 4.

The H_2 conversion efficiency is seen to rise steeply to a maximum of 26.5% at a H_2:N_2 ratio of 0.4, and then decrease progressively as H_2:N_2 increases. The concentration of NH_3 rises to a maximum of 62.7 mol% at a H_2:N_2 ratio of 1.5, and then falls slowly as H_2:N_2 increases. Based on this data, a H_2:N_2 ratio of 1.0 is selected to achieve both a high H_2 conversion efficiency and a high NH_3 product concentration. This ratio is used in subsequent simulation designs.

Table 4 – Comparison of industrial field test data and Aspen Plus simulation results.

Data	Field Data [29]	Simulation Data
Feed composition, mol. frac.		
N_2	0.1986	
H_2	0.6230	
Ar	0.0589	
NH_3	0.0270	
C1	0.0943	
Molar flow, kmol h^{-1}	26409.44	
Pressure drop across bed, MPa	0.17	
Inlet temperature, °C	265	15
Inlet pressure, MPa(abs)	17.1	17.1
Bed 1 inlet temperature, °C	381, 371, 391	394
Bed 1 outlet temperature, °C	519, 519, 512	509
Bed 2 inlet temperature, °C	430, 434, 437	437
Bed 2 outlet temperature, °C	471, 475, 479	476
Bed 3 inlet temperature, °C	411, 411, 416	414
Bed 3 outlet temperature, °C	439, 443, 448	448
NH_3 concentration out, vol%	15.84	15.92

Scaleup of catalyst beds

Having calibrated the Aspen Plus model to simulate real industrial plant performance, the next step is to scale the reactor to a standard commercial scale of 1500 t d^{-1} NH_3. This involves adjusting the catalyst bed dimensions to maintain constant gas residence time.

By stoichiometry, an ammonia production rate of 1500 t d^{-1} requires a hydrogen feed rate of 11 t h^{-1}. Nitrogen is provided as both fresh feed and recycle, with both streams combining at the reactor inlet with a H_2:N_2 molar ratio of 1:1. Adopting a simplified scenario, reactor outlet gas is separated into a liquid ammonia stream and a recycle stream, with 10 mol% of the recycle stream being purged. The fresh nitrogen feed rate and the catalyst bed equivalent diameters are both adjusted incrementally to achieve a H_2:N_2 ratio of 1.0 at the reactor inlet, while maintaining constant gas residence times in each bed. In this scenario, the required N_2 feed rate is 57.3 t h^{-1} (feed H_2:N_2 molar ratio of 2.69:1), and the total bed volume being is increased from 51.85 m^3 (Table 3) to 80.16 m^3 (Table 5).

The resulting NH_3 concentration and temperature profiles within each catalyst bed are shown in Fig. 5. The profiles are seen to be very similar to those in Fig. 3. This confirms that the scaled-up catalyst beds exhibit similar performance to the commercial plant.

Ammonia synthesis reactor performance

The final step in the design process is to incorporate the scaled-up ammonia synthesis reactor into the complete AMMONIA Hierarchy block (Fig. 2), integrated with the lignite-to-hydrogen flowsheet (Fig. 1). The design flowrate of hydrogen from the lignite-to-hydrogen plant is 32.4 t h^{-1}, and the ammonia synthesis reactor is designed to handle 11 t h^{-1} hydrogen, so three ammonia reactors operating in parallel are needed to provide the necessary capacity.

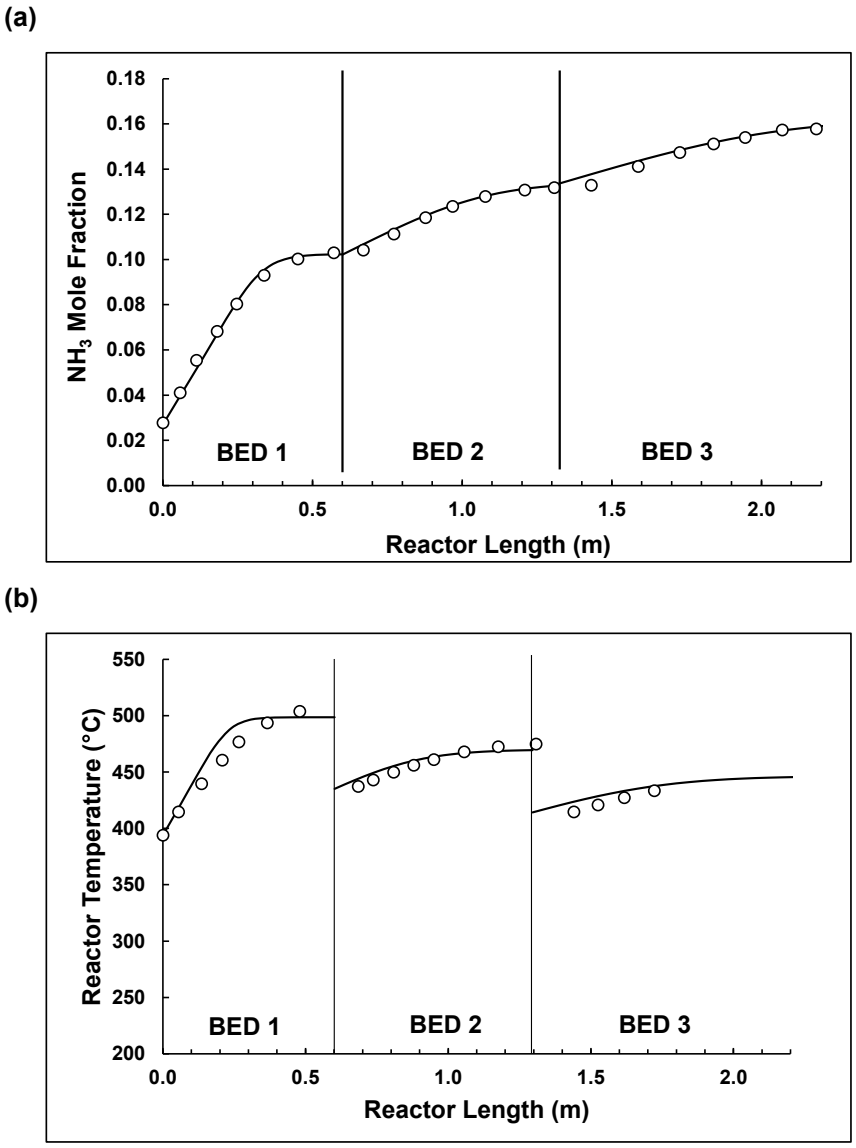

Fig. 3 – Comparison between industrial test and simulation data for (a) ammonia concentration and (b) temperature profiles in each catalyst bed (— Simulation results; ○ Vendor data from Ref. [29]).

The feed rate of H_2 to each ammonia synthesis reactor is set at 10.8 t h^{-1}, and the N_2 feed rate was set at 57.3 t h^{-1}, as in Section 2.5 above. Initially, the catalyst beds were scaled up using a simplified scenario in which 10% of the recycle stream was purged. In the final design, a purge of only 0.7 mol% of the recycle gas is found to be sufficient to prevent accumulation of argon in the system, due to the high purity of the reactant gases (H_2 at 99.999% purity and N_2 at >99.9% purity). However, the simulation is unstable under these conditions and does not converge. This problem is solved by also purging the vapour phase outlet from the second flash unit, which is sent to the gas turbine for combustion of residual H_2 and NH_3. This increases the total purge volume to 1.3 mol% and allows the simulation to converge.

The methodology described in Ref. [15] and its Supplementary Information is used to estimate the total resource requirements and CO_2 emissions intensity associated with production of 32.4 t h^{-1} low-emissions hydrogen from lignite, with all required electricity co-generated on site and conversion of the hydrogen to liquid ammonia. The assumptions involved in estimating the energy intensity of this process are summarised in Table 6.

Results

Considering the performance of a single ammonia synthesis unit, the simulation results for the main streams associated with the AMMONIA Hierarchy block are presented in Table 7. Based on this data, Fig. 6 illustrates a simplified schematic of the system inputs and outputs.

The mass flows of fresh hydrogen and nitrogen in the combined input stream (S-1) are 10.8 t h^{-1} and 57.3 t h^{-1}, respectively, giving a feedstock H_2:N_2 molar ratio of 2.64:1.

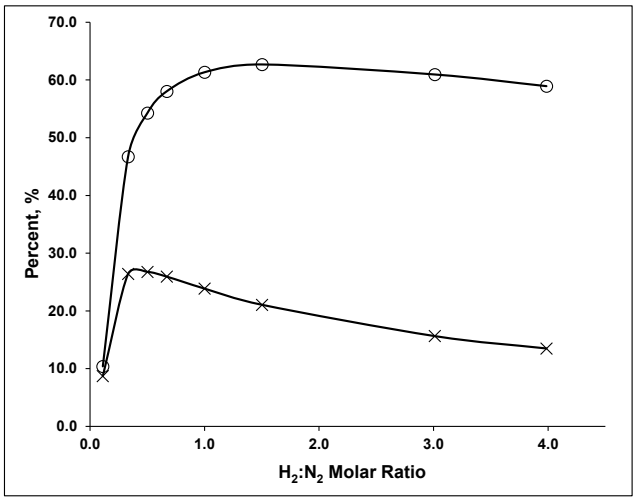

Fig. 4 – Conversion efficiency of H_2 (×) and mol% of NH_3 (◯) as a function of H_2:N_2 ratio.

After mixing with the recycle loop (RECY-4), the H_2:N_2 molar ratio at the reactor inlet (1) is 0.9:1. Liquid ammonia at −3 °C, 2.5 MPa is produced at a purity of 99.1 mol%, at a rate of 59.4 t h^{-1} or 1426 t d^{-1}.

Of the 10.8 t h^{-1} H_2 entering the system, 0.3 t h^{-1} is lost in the combined purge streams and none is present in the liquid ammonia product. Thus, 10.5 t h^{-1} H_2 is converted to NH_3, representing an overall conversion efficiency of 97.2%. The flow of H_2 is 28.2 t h^{-1} at the reactor entry and 17.7 t h^{-1} at the exit, representing a conversion efficiency of 37.2% per pass. This value is higher than anticipated from Fig. 4, which was based on 10 mol% purge from the recycle stream. In this case the purge is only 1.3%, so the additional H_2 recycled to the reactor results in higher conversion efficiency.

The designed ammonia synthesis reactor thus achieves a representative industrial-scale capacity and a high conversion efficiency. The design concept involves three such reactors operating in parallel, to convert 32.4 t h^{-1} H_2 and 171.9 t h^{-1} N_2 into 178.2 t h^{-1} NH_3 at 99.1 mol% purity.

Integration of the AMMONIA Hierarchy block into the larger lignite-to-hydrogen simulation allows the resource requirements and emissions intensity of ammonia production to be estimated. Drawing upon the equivalent data from our earlier study [15], a direct comparison can be made between liquefied hydrogen (LH2) and ammonia (NH3) production. The respective data is presented for comparison in Table 8, with additional details provided in the Supplementary Information.

The first, and most surprising, point to note from these results is that the electrical power requirements for hydrogen liquefaction and ammonia synthesis are essentially identical, at 176.4 MW and 175.5 MW respectively. It was expected that ammonia synthesis would be less energy-intensive than hydrogen liquefaction, but new designs for large-scale hydrogen liquefaction offer significant efficiency improvements [43]. The energy required by COMP1 to compress hydrogen and nitrogen to the Haber-Bosch reaction pressure is 171.9 MW, largely determined by the high mass flow of nitrogen. The two other compressors, COMP2 and COMP3, are tiny in comparison, consuming 2.9 MW and 0.7 MW respectively.

Since the power requirements for hydrogen liquefaction and ammonia synthesis are the same, the lignite feed rate was set as equal in each case to better highlight the differences between the two scenarios. Consequently, the mass flows of inputs and outputs associated with gaseous hydrogen production are also the same.

The LH2 scenario is designed so that a lignite feed rate of 1050 t h^{-1} is sufficient for production of 32.4 t h^{-1} hydrogen and enough electricity to just satisfy the needs of the process (see Table S1 for details). In the NH3 scenario, the same lignite feed rate supports an excess of 26.9 MW electricity production due to combustion of purge gas from the ammonia reactors in the gas turbine. This extra electricity could potentially be used within the process to slightly reduce the amount of lignite feed required and the overall emissions intensity of the process.

In both scenarios, the heat that can be recovered from the steam cycle is sufficient to match the endothermic load within the hydrogen production process (see Table S2 for details). In the NH3 scenario, there is an excess of 148 MW_{th} associated with waste heat from the inlet gas compression system. Normal industrial practice is to use water as the compressor cooling medium, producing hot water that can be used for heat integration [44]. Alternatively, some of this waste heat could be converted to electricity using an organic Rankine cycle system. This is an established industrial process [45], but a more detailed study is required to assess the potential for extra electricity generation in this particular situation.

Since both the LH2 and NH3 scenarios involve the same lignite feed rate, the quantities of CO_2 produced and captured are also the same (see Table S3 for details). As previously described [15], CO_2 capture in the hydrogen production process is mainly accomplished using a two-stage Selexol™ process, which achieves an apparent CO_2 capture efficiency of 91.7%. If required, an additional MDEA capture system can be installed to capture CO_2 from the gas turbine flue gas, increasing the apparent capture efficiency to 99.2%. The same capture efficiencies also apply in the NH3 scenario because combustion of purged H_2 and NH_3 in the gas turbine does not produce CO_2.

The specific emissions intensity (SEI) of producing liquefied hydrogen using only the Selexol™ system for CO_2 capture is

Table 5 – Scaled up bed dimensions for conversion of 11 t h^{-1} hydrogen to ammonia.

Reactor Bed	Volume, m^3	Bed Depth, m	Equiv. Diameter, m	β	Residence Time, s
1	35.46	0.602	8.66	0.5	8.12
2	17.40	0.694	5.65	0.7	5.28
3	27.30	0.916	6.16	0.7	8.68

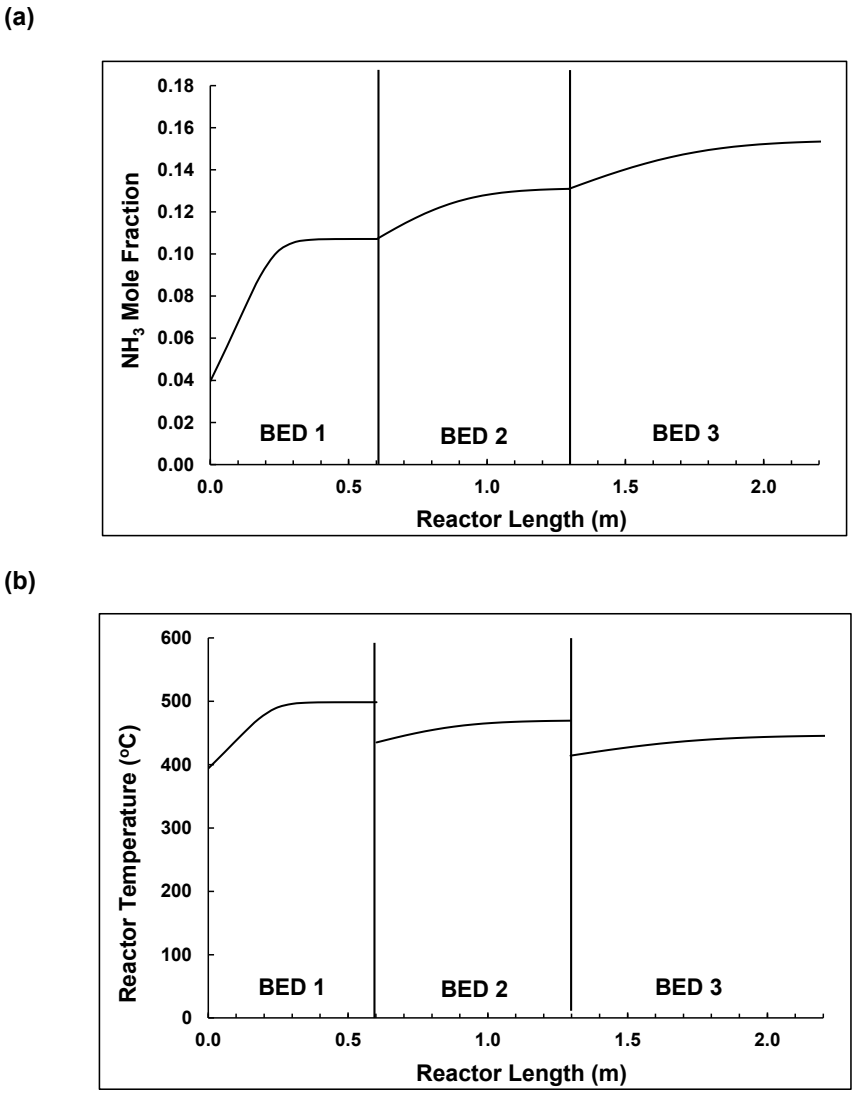

Fig. 5 – Simulation of scaled-up reactor showing (a) ammonia concentration and (b) temperature profile in each catalyst bed.

estimated as 2.73 $kg_{CO2\text{-}e}$ kg_{H2}^{-1}, including fugitive methane emissions during lignite mining. This is consistent with the EU Taxonomy specification for 'sustainable hydrogen', currently set at 3.0 $kg_{CO2\text{-}e}$ kg_{H2}^{-1} [15]. Adding the optional MDEA unit, to conform with a 'net zero by 2050' policy, would further reduce the SEI to 0.30 $kg_{CO2\text{-}e}$ kg_{H2}^{-1}. The results of this study (Table 8) indicate that production of ammonia using a similar process would have a SEI of 0.49 $kg_{CO2\text{-}e}$ kg_{NH3}^{-1} using the Selexol™ system alone, and 0.05 $kg_{CO2\text{-}e}$ kg_{NH3}^{-1} with the optional MDEA unit installed.

Discussion

Significance of this study

The objective of this work is to extend our previous study on production of low emissions hydrogen from Victorian lignite to investigate the relative merits of producing ammonia rather than liquefied hydrogen for export. This comparison required the development of an Aspen Plus simulation of the Haber-Bosch ammonia synthesis process for incorporation into our earlier lignite-to-hydrogen process model.

Despite the widespread industrial use of the Haber-Bosch process, this is the first time that an Aspen Plus simulation has been developed using modified Temkin rate kinetics calibrated to the popular iron-based catalyst, and scaled to representative industrial dimensions using actual plant data. This study is also unusual in that the H_2:N_2 ratio in the reactor feed was selected to maximise H_2 conversion efficiency while minimising the recycle loop volume., rather than simply using the stoichiometric ratio of 3:1. The scaled-up reactor design, calibrated against industrial test data, provides a reasonable simulation of a typical industrial-scale ammonia synthesis plant. Incorporation of this simulation into the larger lignite-to-hydrogen process model enables estimation of the resource and energy requirements of a lignite-to-ammonia process, as well as the associated CO_2 emissions intensity.

Surprisingly, the simulation results show that the electrical power requirement for ammonia synthesis (176.4 MW) is essentially the same as that needed for liquefaction of an equivalent output of hydrogen (175.5 MW). Given that

Table 6 – Electrical and thermal energy requirements of individual unit operations.

Unit operation	Energy requirement	Source
Lignite mining		
Total electrical energy	5.61 $kW_e h\ t^{-1}$ lignite[a]	Plant data from AGL Loy Yang
Lignite drying		
Electrical energy for compression	36.34 $MW_e h\ t^{-1}$ lignite[a]	Model estimate [15]
Additional thermal energy for drying	0.077 $MW_{th} h\ t^{-1}$ lignite[a]	Model estimate [15]
Specific milling energy		
Lignite	6 $kW_e h\ t^{-1}$ lignite[a]	Model estimate [15]
Air Separation Unit		
Electrical energy (air input basis)	0.060 $MW_e h\ t^{-1}$ air	Model estimate [15]
Electrical energy (O_2 output basis)	0.263 $MW_e h\ t^{-1}$ O_2 (@ 95%)	Model estimate [15]
Electrical energy (N_2 output basis)	0.077 $MW_e h\ t^{-1}$ N_2 (@ 98%)	Model estimate [15]
Acid Gas Removal (Selexol™)		
Electrical energy required	0.012 $MW_e h\ t^{-1}$ CO_2	Model estimate [15]
Reboiler duty	0.099 $MW_e h\ t^{-1}$ CO_2	Model estimate [15]
Ammonia chiller		
Cooling load	0.098 $MW_{th} h\ t^{-1}$ CO_2	Model estimate, based on [39]
Reboiler duty	0.147 $MW_{th} h\ t^{-1}$ CO_2	Model estimate, based on [39]
Sour water stripping		
Reboiler duty	0.0245 $MW_{th} h\ t^{-1}$ water	Model estimate [15]
Post-combustion MDEA		
Reboiler duty	1.333 $MW_{th} h\ t^{-1}$ CO_2	Replicated from [40]
CO_2 dehydration (TEG)		
Reboiler duty	1.660 $MW_{th} h\ t^{-1}$ water	Using gas stripping [41]
CO_2 compression		
Compressor duty	0.075 $MW_e h\ t^{-1}$ liquid CO_2	Replicated from [1]
Pressure Swing Adsorption		
Compressor duty	0.5 $MW_e h\ t^{-1}$ H_2	Reported by [42]
Hydrogen pipeline transport		
Compressor duty	1.59 $MW_e h\ t^{-1}$ H_2	Model estimate [15]
Hydrogen liquefaction		
Compressor duty	6 $MW_e h\ t^{-1}$ H_2	Linde design [43]
Ammonia synthesis		
Compressor duty	0.98 $MW_e h\ t^{-1}$ NH_3	Model estimate (current)

[a] Based on as-mined wet lignite.

hydrogen liquefaction plants at the required scale are still only at the conceptual stage, this finding suggests that conversion of hydrogen to ammonia presents a lower technical risk for hydrogen export from Victoria with no additional energy penalty. In fact, this option may provide opportunities for additional electricity production from waste process heat, but a detailed heat integration study is required to quantify this, which is beyond the present scope.

This study finds that 1050 t h^{-1} lignite (LHV 24.91 MJ kg^{-1}) can produce 178.2 t h^{-1} liquid ammonia, equating to a specific energy consumption (SEC) of 146.8 GJ t^{-1}. This compares well with the value of 165.9 GJ t^{-1} reported for the Indian fertiliser industry during the 1990s [46]. This figure is directly comparable to the present study because it includes the energy consumption during mining and preparation of the coal feedstock. Most reports on energy consumption in ammonia production relate to SMR of natural gas, where the SEC ranges from 35 to 41 GJ t^{-1} [47]. However, these values does not take into account the energy involved in extraction, purification and transport of natural gas, or the associated fugitive methane emissions.

This is the first time that the greenhouse gas emissions intensity of ammonia production from lignite have been quantified, accounting for the full production chain from lignite mining to CO_2 sequestration. Following the approach of our previous study [15], two CO_2 capture scenarios are

Table 7 – Stream data for each ammonia synthesis reactor.

Data	S-1	1	6	V	RECY-1	L	V-1	L-1	RECY-4
Temperature, °C	15.2	392.7	452.2	−5	−5	−5	−3	−3	393
Pressure, MPa	2.75	17.1	17.0	16	16	16	25	25	17.1
Mass flow, t h^{-1}	68.1	491.2	491.3	427.1	4.3	64.0	4.6	59.4	423.0
H_2 mass flow, t h^{-1}	10.8	28.2	17.7	17.6	0.2	0.0	0.1	0	17.4
N_2 mass flow, t h^{-1}	57.3	443.7	394.9	390.2	3.9	4.7	3.8	0.9	386.3
NH_3 mass flow, t h^{-1}	0	19.3	78.7	19.3	0.2	59.3	0.7	58.5	19.3
Ar mass flow, t h^{-1}	0.00002	0.001	0.001	0.001	0	0	0	0	0

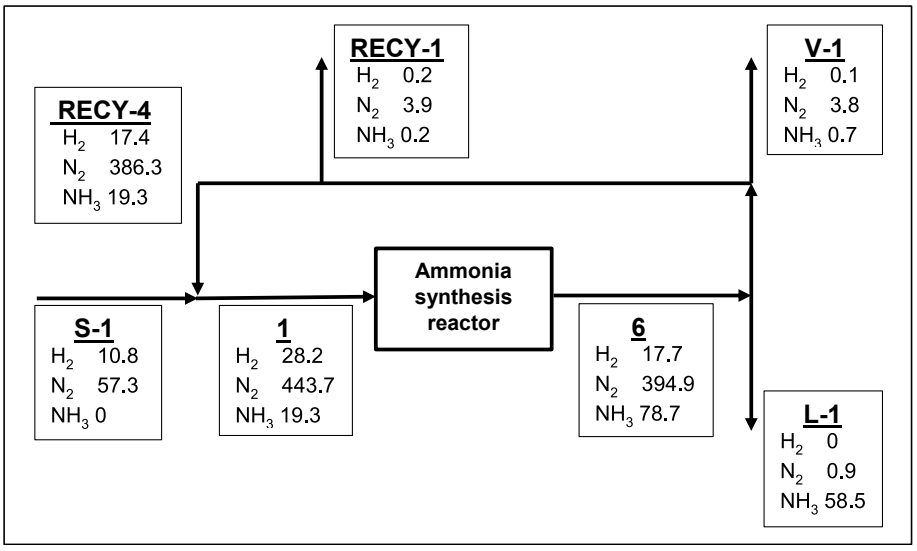

Fig. 6 – Simplified mass flows around each ammonia synthesis reactor (t h^{-1}).

considered. In the baseline scenario, all CO_2 capture is accomplished in the main Selexol™ acid gas recovery plant, operating at an apparent capture efficiency of 91.7%. The SEI of ammonia production in this scenario is 0.49 $kg_{CO2\text{-}e}$ kg_{NH3}^{-1}, including fugitive methane emissions during lignite mining.

Table 8 – Summary of process inputs and outputs for each scenario.

	Scenario	
Process inputs	LH2	NH3
As-mined lignite feed rate, t h^{-1}	1050	1050
Pulverised lignite feed rate, t h^{-1}	466.7	466.7
Oxygen flowrate, t h^{-1}	345	345
Nitrogen flowrate, t h^{-1}	–	171.9
Process outputs		
Liquefied H_2 production, t h^{-1}	32.4	–
NH_3 production, t h^{-1}	–	178.2
CO_2 captured (Selexol™ only), t h^{-1}	1170.9	1170.9
CO_2 captured (with MDEA), t h^{-1}	1249.6	1249.6
Sulphur production, t h^{-1}	1.1	1.1
Water from lignite dryer, t h^{-1}	584	584
Slag production, t h^{-1}	10.8	10.8
Fugitive CH_4 emissions, t h^{-1}	0.012	0.012
Electrical power		
Power for H_2 production, MW_e	304.9	304.9
Power for H_2 liquefaction, MW_e	176.4	–
Power for NH_3 synthesis, MW_e	–	175.5
Total power required, MW_e	**481.3**	**480.1**
Total power generated, MW_e	481	507
Excess capacity, MW_e	−0.3	26.9
Thermal power		
Thermal power required, MW_{th}	−549	−549
Thermal power recovered, MW_{th}	554	554
Extra thermal power available, MW_{th}	0	148
Apparent capture efficiency of CO_2 in syngas, %		
Selexol™ only	91.7	91.7
Selexol™ plus MDEA	99.2	99.2
Emissions intensity, kg CO_2-e kg^{-1} H_2 or NH_3		
Selexol™ only	2.73	0.49
Selexol™ plus MDEA	0.30	0.05

There is currently no agreed specification set for emissions from blue ammonia production, but the hydrogen used as feedstock meets the EU Taxonomy specification for 'sustainable hydrogen' and no further emissions are produced in ammonia production, so the proposed lignite-to-ammonia process should qualify as 'sustainable' or 'low-emission'.

In the second CO_2 capture scenario, the emissions intensity is reduced further by fitting a MDEA adsorption unit to the gas turbine flue gas stream. It is anticipated that this option may become necessary as allowable emissions limits are progressively lowered over the coming decades. The MDEA unit allows hydrogen to be produced with a SEI of 0.30 $kg_{CO2\text{-}e}$ kg_{H2}^{-1}, and ammonia at 0.05 $kg_{CO2\text{-}e}$ kg_{NH3}^{-1}. As previously shown, the process could then be made net-zero by co-gasification with ≤1.4 wt% biomass [15].

There is a lack of industrial data that can be directly compared with the proposed lignite-to-ammonia process. The SEI of large coal-based ammonia plants in China is reported to be 9.0 $kg_{CO2\text{-}e}$ kg_{NH3}^{-1} [13], but CCS is not used. In Japan, Ube Corporation produces 1000 t d^{-1} ammonia from coal but does not capture CO_2 emissions. In the USA, Coffeyville Resources produces 1,300 t d^{-1} ammonia from petroleum coke, and captures 650,000 t y^{-1} CO_2 [48], but the emissions intensity has not been reported.

However, it has been reported that the SEI of SMR is 3.0 $kg_{CO2\text{-}e}$ kg_{NH3}^{-1} [13] and that this could be reduced to 0.44–0.54 $kg_{CO2\text{-}e}$ kg_{NH3}^{-1} with 90% CO_2 capture (including fugitive methane emissions [14]. On this basis, the estimated 0.49 $kg_{CO2\text{-}e}$ kg_{NH3}^{-1} for the proposed lignite-to-ammonia process, with 91.7% CO_2 capture using Selexol™, compares favourably with next-generation SMR processes.

Victorian lignite is actually more advantageous than natural gas for low-emissions ammonia production, because it has inherently low fugitive methane emissions and a stable, low cost of production. It also has the advantage of proximity to massive, high quality CO_2 storage reservoirs. Thus, the proposed lignite-to-ammonia process seems to offer significant advantages for the emerging clean hydrogen market.

Table 9 – Renewable energy required for production of 32.4 t h^{-1} H_2 and conversion to liquid hydrogen or ammonia.

Unit Operation	Energy Intensity	G-LH2, MW	G-NH3, MW	Reference
RO seawater desalination	4 kWh t^{-1} purified H_2O	2.6	2.6	[50,51]
Electrolysis	1.08 * 50 MWh t^{-1} H_2	1749.6	1749.6	[52]
N_2 production by PSA	110 kWh t^{-1} N_2	18.9	18.9	[53]
H_2 liquefaction	6 MWh t^{-1} H_2	176.4	–	[43]
H_2, N_2 compression	0.98 MWh t^{-1} NH_3	–	175.2	This study
Totals		**1947.5**	**1946.3**	

Application to green hydrogen and ammonia production

Given public scepticism around production of low emission hydrogen from fossil fuels with CCS, it of interest to compare the findings of this study with the option of producing the same quantity of ammonia using renewable energy.

Using renewable energy, pure H_2 is produced by electrolysis of water which is typically produced by desalination of seawater using reverse osmosis (RO). By stoichiometry, 1 tonne of H_2 requires 9 tonnes water, and the typical water recovery from seawater desalination is 45% [49], making a total water requirement of 20 t water t^{-1} H_2. Typical energy intensity of seawater desalination by RO is around 4 kWh t^{-1} purified water [50,51]. Water electrolysis using proton exchange membrane (PEM) technology is expected to have a SEC of 50 kWh t^{-1} H_2 by 2030, but about 8% extra energy is required to account for the auxiliary load which must be met before hydrogen can be generated, and the losses through the power electronics [52]. Pure N_2 can be extracted from air using PSA, with a SEC of 110 kWh t^{-1} N_2 [53]. Next-generation hydrogen liquefiers with capacities of hundreds of tonnes per day are expected to have SEC close to or below 6 kWh kg_{LH2}^{-1} [43]. The present study has found that the SEC for compression of H_2 and N_2 to the Haber-Bosch reaction pressure is 0.98 MWh t_{NH3}^{-1} produced. Using this data, Table 9 summarises the electrical energy required to produce 32.4 t h^{-1} H_2 via electrolysis and convert it to either liquefied hydrogen (G-LH2) or liquid ammonia (G-NH3). The total energy required to produce 178.2 t h^{-1} green ammonia is 1946.3 MW, equating to a SEI of 10.9 MWh t_{NH3}^{-1}. This is consistent with a previously published estimate of 10.6 MWh t_{NH3}^{-1} [54].

These estimates of electrical energy consumption are based on 100% supply availability. A significantly larger installed capacity of renewable energy generation is needed to account for supply intermittency. For example, the availability of wind energy in Victoria averages 36% throughout the year [55], so provision of 1946.3 MW for ammonia production would require a wind farm with a total nameplate capacity of 5.4 GW. Currently, the largest wind farm in Victoria is the 420 MW Macarthur installation, which has 140 turbines over an area of 5,500 ha. Installation of 5.4 GW wind turbine capacity for green ammonia production in Victoria would require the equivalent of 13 Macarthur wind farms, potentially requiring an area of over 72,000 ha.

Apart from the very large wind turbine capacity needed to support this output of green ammonia, the feasibility of sourcing sufficient electrolyser capacity is questionable. The estimated global installed capacity of electrolysers in 2021 was 600 MW, in mostly small and individually manufactured plants [56]. The industry is not configured for production volumes beyond several thousand parts per year [57], and the exotic materials required (e.g. iridium, yttrium, platinum, strontium, and graphite) are in limited supply [58]. It therefore seems likely that the global capacity to produce green ammonia will be constrained over the next several decades.

In contrast, gasification of coal and lignite is a very well established, conventional technology with a proven track record for reliable production of valuable industrial chemicals and fuels. Gasification technologies are available from numerous vendors, and are well suited for production of hydrogen at the scale investigated in this study. Likewise, CCS is now well established. There are currently 114 active commercial CO_2 injection enhanced oil recovery (EOR) projects in the United States that collectively inject over 1.8 Mt y^{-1} CO_2 and produce over 280,000 barrels of oil per day [59]. There over 40 sites where EOR has been used to safely and securely store captured CO_2 underground, and continuous monitoring has verified that the wells are intact and secure. There are currently 30 full-scale projects operating globally and 164 new projects in development, with a total storage capacity of 241.6 Mt y^{-1} [60]. CCS has demonstrably been proven to be a safe and effective climate mitigation tool.

In Victoria, the CarbonNet Project has validated that safe CO_2 storage sites are available in the near-offshore region of the Gippsland Basin [61]. In addition, ESSO Australia recently announced the South Eastern Australia CCS Hub, which from 2024 will use existing gas extraction infrastructure to store CO_2 in the depleted Bream reservoir, located 46 km offshore in Bass Strait. As ESSO's oil and gas fields in Bass Strait reach the end of their working lives, they can be converted to CO_2 storage reservoirs, with potential capacity of 50–300 billion tonnes [62].

Based on resource requirements and availability, production of blue ammonia by lignite gasification with CCS in Victoria has significant advantages compared to green ammonia. Gasification of lignite with CCS has much greater capacity than electrolysis to be deployed at large scale, so blue ammonia from Victorian lignite is well placed to play a role in the global transition to low emissions fuels.

Conclusion

This study extends our previous study, on production of low emissions hydrogen from Victorian lignite, to examine production of ammonia rather than liquefied hydrogen as a

hydrogen carrier for export. The objective of this study is to evaluate the resource requirements and emissions intensity associated with ammonia production by lignite gasification with CCS. This involves development of an Aspen Plus simulation of the Haber-Bosch ammonia synthesis process, and running it within our earlier lignite-to-hydrogen process model.

Surprisingly, the simulation results show that the electrical power requirement for ammonia synthesis is essentially the same as that needed for liquefaction of an equivalent output of hydrogen. On this basis both options are equally attractive, although ammonia synthesis is at a higher level of technological maturity than large-scale hydrogen liquefaction.

This study shows that blue ammonia can be produced from Victorian lignite with very low carbon intensity (0.49 $kg_{CO2\text{-}e}$ kg_{NH3}^{-1}) equivalent to that of with next-generation SMR + CCS processes. If required, the emission intensity can be reduced to 0.05$kg_{CO2\text{-}e}$ kg_{NH3}^{-1} with a post-combustion MDEA system, and then made carbon neutral by co-gasification with $\leq$1.4% biomass. This suggests that Victoria is well placed to become a significant supplier of low emissions ammonia to the world market, consistent with global emissions reductions targets over the next few decades.

A limitation of this study is that the treatment of thermal energy flows is restricted to satisfying process demands using high-value heat from the gasifier, and does not address utilisation of the excess heat generated by the exothermic ammonia synthesis reaction. This heat could potentially be used to generate electricity for use within the plant, thereby reducing the load on the gasifier and gas treatment system, or for sale off-site. Further research is recommended on recovery of energy from the low grade waste heat streams and opportunities for additional electricity generation using the organic Rankine cycle.

Role of funding source

Australian Carbon Innovation (ACI) is a private member-based company that provides funding for R&D of innovative carbon-based technologies in Australia, and encourages public dissemination of the findings. As well as providing funding, ACI also played a collaborative role in this project, assisting Monash University with the literature review and drafting of the manuscript.

Declaration of competing interest

The authors declare that they have no known competing financial interests or personal relationships that could have appeared to influence the work reported in this paper.

Acknowledgements

Funding for this project was provided by Australian Carbon Innovation (ACI), a not-for-profit private member-based company, with the support of the Victorian Government.

Appendix A. Supplementary data

Supplementary data to this article can be found online at https://doi.org/10.1016/j.ijhydene.2023.06.098.

REFERENCES

[1] Hydrogen Council. Hydrogen scaling up. 2017. https://hydrogencouncil.com/en/study-hydrogen-scaling-up. [Accessed 8 December 2022].
[2] Mokhatab S, Mak JY, Valappil J, Wood DA. Handbook of liquefied natural gas. Gulf Professional Publishing.; 2013. p. 624. ISBN 0124046452.
[3] Juangsa FB, Irhamna AR, Aziz M. Production of ammonia as potential hydrogen carrier: review on thermochemical and electrochemical processes. Int J Hydrogen Energy 2021;46(27):14455–77. https://doi.org/10.1016/j.ijhydene.2021.01.214.
[4] Yoshino Y, Harada E, Inoue K, Yoshimura K, Yamashita S, Hakamada K. Feasibility study of "CO_2 free hydrogen chain" utilizing Australian brown coal linked with CCS. Energy Proc 2012;29:701–9. https://doi.org/10.1016/j.egypro.2012.09.082.
[5] Kamiya S, Nishimura M, Harada E. Study on introduction of CO_2 free energy to Japan with liquid hydrogen. Phys Procedia 2015;67:11–9. https://doi.org/10.1016/j.phpro.2015.06.004.
[6] HESC. In: Successful completion of pilot project report; 2022. https://www.hydrogenenergysupplychain.com/report-successful-completion-of-the-hesc-pilot-project;. [Accessed 8 December 2022].
[7] Challenge Zero. Development of a technology for large-scale storage and transportation of hydrogen, https://www.challenge-zero.jp/en/casestudy/647 [accessed 8 December 2022].
[8] Rao PC, Yoon M. Potential liquid-organic hydrogen carrier (LOHC) systems: a review on recent progress. Energies 2020;13(22):6040. https://doi.org/10.3390/en13226040.
[9] Ghavam S, Vahdati M, Wilson I, Styring P. Sustainable ammonia production processes. Front Energy Res 29 March 2021. https://doi.org/10.3389/fenrg.2021.580808.
[10] Muraki S. Development of technologies to utilize green ammonia in energy market. In: 2018 NH3 fuel conference. Powerpoint presentation; 2018. https://www.ammoniaenergy.org/wp-content/uploads/2021/02/AEA-Imp-Con-01Nov18-Shigeru-Muraki-Keynote-Address.pdf;. [Accessed 8 December 2022].
[11] Erisman JW, Sutton MA, Galloway J, Klimont Z, Winiwarter W. How a century of ammonia synthesis changed the world. Nat Geosci 2008;1(10):636–9. https://doi.org/10.1038/ngeo325.
[12] International Energy Agency. Ammonia technology roadmap. 2021. https://www.iea.org/reports/ammonia-technology-roadmap. [Accessed 8 December 2022].
[13] Zhang W-f, Dou Z-x, He P, Ju X-T, Powlson D, Chadwick D, et al. New technologies reduce greenhouse gas emissions from nitrogenous fertilizer in China. Proc Natl Acad Sci USA 2013;110:8375–80. https://doi.org/10.1073/pnas.1210447110.
[14] Stocks M, Fazeli R, Hughes L, Beck FJ. Global emissions implications from co-combusting ammonia in coal fired power stations: an analysis of the Japan-Australia supply chain. J Clean Prod 2022;336:130092. https://doi.org/10.1016/j.jclepro.2021.130092.
[15] Kibria MA, McManus D, Bhattacharya S. Options for net zero emissions hydrogen from Victorian lignite. Part 1: gaseous and liquefied hydrogen. Int J Hydrogen Energy 2023. https://doi.org/10.1016/j.ijhydene.2023.04.213.

[16] Appl M. Ammonia, 2. Production processes. Ullmann's Encyclopedia of Industrial Chemistry 2000. https://doi.org/10.1002/14356007.o17_o02.
[17] Andersson J, Lundgren J. Techno-economic analysis of ammonia production via integrated biomass gasification. Appl Energy 2014;130:484–90. https://doi.org/10.1016/j.apenergy.2014.02.029.
[18] Arora P, Hoadley AF, Mahajani SM, Ganesh A. Small-scale ammonia production from biomass: a techno-enviro-economic perspective. Ind Eng Chem Res 2016;55:6422–34. https://doi.org/10.1021/acs.iecr.5b04937.
[19] Aziz M, Putranto A, Biddinika MK, Wijayanta AT. Energy-saving combination of N_2 production, NH_3 synthesis, and power generation. Int J Hydrogen Energy 2017;42:27174–83. https://doi.org/10.1016/j.ijhydene.2017.09.079.
[20] Darmawan A, Ajiwibowo MW, Tokimatsu K, Aziz M. Efficient co-production of power and ammonia from black liquor. Int J Hydrogen Energy 2020;45:34437–48. https://doi.org/10.1016/j.ijhydene.2020.02.196.
[21] Ishaq H, Dincer I. Dynamic modelling of a solar hydrogen system for power and ammonia production. Int J Hydrogen Energy 2021;46:13985–4004. https://doi.org/10.1016/j.ijhydene.2021.01.201.
[22] Dyson D, Simon J. Kinetic expression with diffusion correction for ammonia synthesis on industrial catalyst. Ind Eng Chem Fundam 1968;7:605–10. https://doi.org/10.1021/i160028a013.
[23] Azarhoosh M, Farivar F, Ebrahim HA. Simulation and optimization of a horizontal ammonia synthesis reactor using genetic algorithm. RSC Adv 2014;4:13419–29. https://doi.org/10.1039/C3RA45410J.
[24] Shamiri A, Aliabadi N. Modeling and performance improvement of an industrial ammonia synthesis reactor. Chemical Engineering Journal Advances 2021;8:100177. https://doi.org/10.1016/j.ceja.2021.100177.
[25] Suhan MB, Hemal MN, Choudhury MS, Mazumder MA, Islam M. Optimal design of ammonia synthesis reactor for a process industry. Journal of King Saud University-Engineering Sciences 2022 Jan 1;34(1):23–30. https://doi.org/10.1016/j.jksues.2020.08.004.
[26] Araújo A, Skogestad S. Control structure design for the ammonia synthesis process. Comput Chem Eng 2008;32:2920–32. https://doi.org/10.1016/j.compchemeng.2008.03.001.
[27] Yoshida M, Ogawa T, Imamura Y, Ishihara KN. Economies of scale in ammonia synthesis loops embedded with iron-and ruthenium-based catalysts. Int J Hydrogen Energy 2021 Aug 18;46(57):28840–54. https://doi.org/10.1016/j.ijhydene.2020.12.081.
[28] Rossetti I, Tripodi A, Tommasi M, Ramis G. Conceptual design of a process for hydrogen production from waste biomass and its storage in form of liquid ammonia. Int J Hydrogen Energy 2023. https://doi.org/10.1016/j.ijhydene.2023.01.261.
[29] El-Gharbawy M, Shehata W, Gad F. Ammonia converter simulation and optimization based on an innovative correlation for (Kp) prediction. J Univ Shanghai Sci Technol 2021;35:323–37. ISSN: 1007-6735.
[30] Dybkjaer I. Ammonia production processes. In: Nielsen A, editor. Ammonia: catalysis and manufacture. Berlin, Heidelberg: Springer; 1995. p. 199–327. https://doi.org/10.1007/978-3-642-79197-0_6.
[31] Sueyama T. Features and practical use of Texaco coal gasification process. Coal science symposium and 91st special meeting on coke, osaka (Japan), 7-8 nov 1991. In: Proceedings of the joint meeting of the fuel society of Japan; 1991.
[32] Stork K, Wiles CF, Mathur GK. Ammonia production using the Texaco coal gasification process. Nitrogen 1986;(160):39–50.
[33] Rath LK, Chou VH, Kuehn NJ. Assessment of hydrogen production with CO_2 capture volume 1: baseline state-of-the-art plants. National Energy Technology Laboratory (NETL), Pittsburgh, PA, Morgantown, WV; 2011. https://www.osti.gov/servlets/purl/1767148. [Accessed 8 December 2022].
[34] Jones D, Bhattacharyya D, Turton R, Zitney SE. Optimal design and integration of an air separation unit (ASU) for an integrated gasification combined cycle (IGCC) power plant with CO_2 capture. Fuel Process Technol 2011;92:1685–95. https://doi.org/10.1016/j.fuproc.2011.04.018.
[35] Yu B-Y, Chien I-L. Design and economic evaluation of a coal-based polygeneration process to coproduce synthetic natural gas and ammonia. Ind Eng Chem Res 2015;54:10073–87. https://doi.org/10.1021/acs.iecr.5b02345.
[36] Zhang H, Wang L, Maréchal F, Desideri U. Techno-economic comparison of green ammonia production processes. Appl Energy 2020;259:114135. https://doi.org/10.1016/j.apenergy.2019.114135.
[37] Elnashaie S, Mahfouz A, Elshishini S. Digital simulation of an industrial ammonia reactor. Chem Eng Process: Process Intensif 1988;23:165–77. https://doi.org/10.1016/0255-2701(88)80013-8.
[38] Elnashaie SS, Abashar ME, Al-Ubaid AS. Simulation and optimization of an industrial ammonia reactor. Ind Eng Chem Res 1988;27:2015–22. https://doi.org/10.1021/ie00083a010.
[39] Mansouri R, Boukholda I, Bourouis M, Bellagi A. Modelling and testing the performance of a commercial ammonia/water absorption chiller using Aspen-Plus platform. Energy 2015;93:2374–83. https://doi.org/10.1016/j.energy.2015.10.081.
[40] Aspen Technology. Rate-based model of the CO_2 capture process by MDEA using aspen plus. Cambridge, MA, USA: Aspen Technology Inc; 2016. https://pdfcoffee.com/enrtl-rk-rate-based-mdea-model-pdf-free.html. [Accessed 8 December 2022].
[41] Sakheta A, Zahid U. Process simulation of dehydration unit for the comparative analysis of natural gas processing and carbon capture application. Chem Eng Res Des 2018;137:75–88. https://doi.org/10.1016/j.cherd.2018.07.004.
[42] Lee D-Y, Elgowainy A. By-product hydrogen from steam cracking of natural gas liquids (NGLs): potential for large-scale hydrogen fuel production, life-cycle air emissions reduction, and economic benefit. Int J Hydrogen Energy 2018;43(43):20143–60. https://doi.org/10.1016/j.ijhydene.2018.09.039.
[43] Krasae-In S. Optimal operation of a large-scale liquid hydrogen plant utilizing mixed fluid refrigeration system. Int J Hydrogen Energy 2014;39:7015–29. https://doi.org/10.1016/j.ijhydene.2014.02.046.
[44] Kirova-Yordanova Z. Exergy analysis of industrial ammonia synthesis. Energy 2004 Oct 1;29(12–15):2373–84. https://doi.org/10.1016/j.energy.2004.03.036.
[45] Tchanche BF, Lambrinos G, Frangoudakis A, Papadakis G. Low-grade heat conversion into power using organic Rankine cycles–A review of various applications. Renew Sustain Energy Rev 2011 Oct 1;15(8):3963–79. https://doi.org/10.1016/j.rser.2011.07.024.
[46] Schumacher K, Sathaye J. India's fertilizer industry: productivity and energy efficiency, report LBNL-41846. Berkley, CA: Lawrence Berkeley National Laboratory; 1999. https://www.osti.gov/servlets/purl/764326. [Accessed 22 March 2023].
[47] Rafiqul I, Weber C, Lehmann B, Voss A. Energy efficiency improvements in ammonia production—perspectives and

uncertainties. Energy 2005 Oct 1;30(13):2487–504. https://doi.org/10.1016/j.energy.2004.12.004.
[48] Barkley N. Petroleum coke gasification based ammonia plant. AIChE 51st annual safety in ammonia plants and related facilities symposium, Vancouver, Canada 2006.
[49] Gude VG. Energy consumption and recovery in reverse osmosis. Desalination Water Treat 2011;36:239–60. https://doi.org/10.5004/dwt.2011.2534.
[50] Ghaffour N, Missimer TM, Amy GL. Technical review and evaluation of the economics of water desalination: current and future challenges for better water supply sustainability. Desalination 2013;309:197–207. https://doi.org/10.1016/j.desal.2012.10.015.
[51] Kim J, Park K, Yang DR, Hong S. A comprehensive review of energy consumption of seawater reverse osmosis desalination plants. Appl Energy 2019;254:113652. https://doi.org/10.1016/j.apenergy.2019.113652.
[52] Haywood JA. The economics of producing H_2 from electrolysis in Victoria. CSIRO, Australia. In: Options for production of low cost CO_2-free hydrogen from Victorian Brown coal; 2018. https://www.acinnovation.com.au/aci-reports. [Accessed 8 December 2022].
[53] Morgan E, Manwell J, McGowan J. Wind-powered ammonia fuel production for remote islands: a case study. Renew Energy 2014;72:51–61. https://doi.org/10.1016/j.renene.2014.06.034.
[54] Smith C, Hill AK, Torrente-Murciano L. Current and future role of Haber–Bosch ammonia in a carbon-free energy landscape. Energy Environ Sci 2020;13(2):331–44. https://doi.org/10.1039/C9EE02873K.
[55] Australian Energy Market Operator. National transmission network development plan. 2016 Dec. p. 110. https://aemo.com.au/-/media/files/electricity/nem/planning_and_forecasting/ntndp/2016/report/2016-national-transmission-network-development-plan.pdf?la=en&hash=6711A86D8DFD27BA8491A3B5A07A02DE. [Accessed 8 December 2022].
[56] Odenweller A, Ueckerdt F, Nemet GF, Jensterle M, Luderer G. Probabilistic feasibility space of scaling up green hydrogen supply. Nat Energy 2022;7:854–65. https://doi.org/10.1038/s41560-022-01097-4.
[57] Ayers K, Danilovic N, Ouimet R, Carmo M, Pivovar B, Bornstein M. Perspectives on low-temperature electrolysis and potential for renewable hydrogen at scale. Annu Rev Chem Biomol Eng 2019;10:219–39. https://doi.org/10.1146/annurev-chembioeng-060718-030241.
[58] Badgett A, Brauch J, Buchheit K, Hackett G, Li Y, Melaina M, et al. Water electrolyzers and fuel cells supply chain-supply chain deep dive assessment. USDOE Office of Policy; 2022. https://www.energy.gov/sites/default/files/2022-02/Fuel%20Cells%20%26%20Electrolyzers%20Supply%20Chain%20Report%20-%20Final.pdf. [Accessed 8 December 2022].
[59] Saini D. Simultaneous CO_2-EOR and storage projects. In: Engineering aspects of geologic CO_2 storage. SpringerBriefs in petroleum geoscience & engineering. Springer; 2017. p. 11–9. https://doi.org/10.1007/978-3-319-56074-8_2.
[60] Global CCS Institute. In: Global status of CCS 2022; 2022. https://www.globalccsinstitute.com/resources/global-status-of-ccs-2022. [Accessed 23 March 2023].
[61] Earth Resources. The CarbonNet project. State Government of Victoria, https://earthresources.vic.gov.au/projects/carbonnet-project [accessed 8 December 2022].
[62] The South East Australia carbon capture Hub, https://www.exxonmobil.com.au/energy-and-environment/energy-resources/upstream-operations/the-south-east-australia-carbon-capture-hub [accessed 8 December 2022].